Cancellation of Air-Induced Passive Intermodulation in FDD MIMO Systems: Low-Complexity Cascade Model and Measurements

Vesa Lampu*, Lauri Anttila*, Matias Turunen*, Marko Fleischer†, Jan Hellmann†, and Mikko Valkama*
*Department of Electrical Engineering, Tampere University, Tampere, Finland
†Nokia Mobile Networks, Ulm, Germany
vesa.lampu@tuni.fi

***Abstract*— This paper presents a low-complexity cascade scheme for identifying and cancelling air-induced passive intermodulation (PIM) in multiple-input multiple-output (MIMO) frequency division duplex (FDD) transceivers. PIM is in general generated by nonlinear passive devices, while in the special case of air-induced PIM, the interference stems from objects outside the transceiver system. In FDD systems, the induced intermodulation products may cause severe self-interference to the receiver (RX) band. This work presents a general solution to air-induced PIM mitigation, allowing for any number of parallel transceiver chains, unlike previous works. Moreover, the utilization of spline-interpolated lookup table (LUT) and least mean squares (LMS)-based parameter adaptation allows for a great reduction in the overall complexity of the cancellation engine, compared to previous works. This is achieved without compromising the cancellation performance, as is evidenced in real-life RF measurements at 5G NR band n3.**

***Keywords*— 5G, carrier aggregation, duplexing, interference cancellation, nonlinear systems, passive intermodulation, splines**

I. Introduction

To increase the throughput and capacity of modern wireless communication devices, the 5G NR specifications [1] incorporate carrier aggregation (CA) technology leveraging the transmission of multiple component carriers (CCs), which can be allocated within the available spectrum contiguously or non-contiguously. In addition, the 5G NR specifications continue to support the frequency division duplex (FDD), where the transmitter (TX) and receiver (RX) operate simultaneously on different center frequencies, as the duplexing scheme in certain frequency range (FR)-1 bands. In the event that non-contiguously allocated CCs experience a shared nonlinearity, intermodulation products are generated, which can fall on the RX band in FDD operation, as shown in Fig. 1, possibly thus desensitizing the RX. When the source of such intermodulation is a passive device, the distortion is referred to as passive intermodulation (PIM), which, in general, can be generated by loose connections, switches, filters, and – as is the case in this work – external metallic objects in the radiation field of the antennas, which we refer to as air-induced PIM.

The simplest solutions to the mitigation of the PIM issue are to back-off the TX power, or to utilize linear components [2], [3]. These have the unfortunate consequences of lowering the coverage and power efficiency of the TX, and increasing the manufacturing costs, respectively. Furthermore, in the air-induced PIM scenarios, the source of the distortion may be part of the built environment, and therefore impossible to remove. Hence, PIM cancellation techniques have been sought in literature.

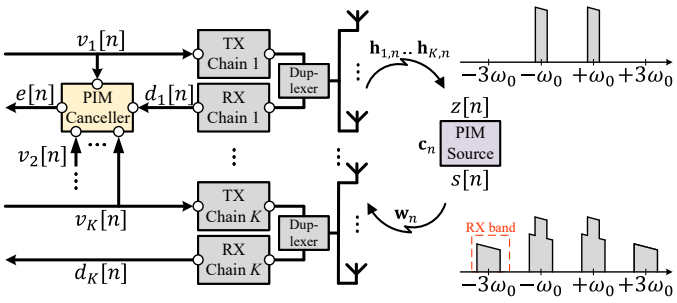

Fig. 1. System model, where K parallel transceiver chains transmit two CCs and receive air-induced PIM distortion stemming from the external PIM source. Some basic modeling notations are also shown.

The PIM suppression can generally be carried out in the analog or digital domain. In analog domain [2], [3], [4], [5], the PIM distortion can be mitigated by injecting a compensation signal [2] or by an artificial PIM source [3], [4], while a general framework for adaptive feedforward cancellation was introduced in [5]. In the digital domain techniques [6], [7], [8], within which this work also falls into, baseband modeling of the interfering PIM distortion is utilized in two concurrent CC [6], and up to three CC [7] cases, while the work in [8] considered the co-exitestence of nonlinear power amplifiers (PAs) with two CCs.

The previous works in MIMO air-induced PIM successfully cancelled PIM in a challenging rank-2 MIMO operation with two concurrent CCs, (i.e., four distinct signals), while the lowered complexity modeling assumed memoryless, single-tap channel responses [9]. While this may be sufficient in many scenarios, in this work, we extend the PIM modeling to support any K number of parallel MIMO streams, and to cope with channel responses with potential memory effects by leveraging a Wiener-Hammerstein-type cascaded model, where the nonlinear response is modeled with a spline-interpolated lookup table (LUT). These, paired with a low-complexity least mean squares (LMS) parameter adaptation, leads to a very low-complexity and implementation feasible general solution to model and cancel the air-induced PIM. RF measurements conducted with real-life hardware at the 5G NR band n3 (the 1.8 GHz band) indicate that high cancellation fidelity is attained through the proposed solution, with the proposed solution being capable of even outperforming the more complex reference models in high

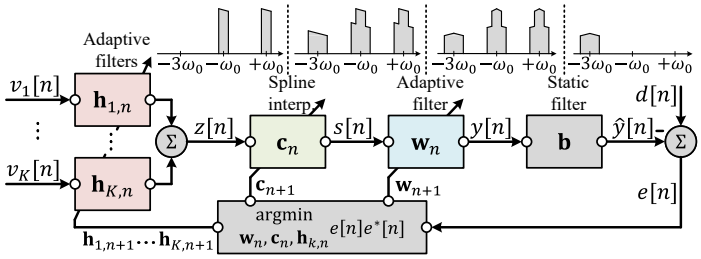

Fig. 2. Block diagram of the proposed cancellation method and parameter adaptation, showing also the conceptual spectra of the main path signals.

TX power scenarios.

II. Proposed Cancellation Method

Here, we describe the proposed cancellation method for a system where an air-induced PIM source interferes with the RX band, as shown in Fig. 1, using complex-valued baseband modeling. We consider a dual-carrier rank-K FDD MIMO operation, i.e., there are K TX chains each transmitting two physical CCs, denoted as $x_{k,1}[n]$ and $x_{k,2}[n]$, for $k = 1, 2, \cdots, K$, and the CCs are transmitted at baseband frequencies $-\omega_0$ and $+\omega_0$, respectively. Further, the operating frequency of each RX chain is defined as the lower third order intermodulation frequency $-3\omega_0$. A block diagram of the proposed method is shown in Fig. 2, which follows a Wiener-Hammerstein-type approach, where a nonlinear block is both preceded and followed by a linear filter. The proposed processing can be applied to each receiver independently.

A. Main Path

We first define summed composite signals $v_k[n]$, for $k = 1, 2, \cdots, K$ at each TX chain as

$$v_k[n] = x_{k,1}[n]e^{-j\omega_0 n} + x_{k,2}[n]e^{+j\omega_0 n}. \tag{1}$$

The K composite signals propagate through wireless channels to the PIM source where they combine to produce the PIM source input signal $z[n]$ as

$$z[n] = \sum_{k=1}^{K} \mathbf{h}_{k,n}^T \mathbf{v}_{k,n}, \tag{2}$$

where $\mathbf{h}_{k,n} \in \mathbb{C}^{H\times 1}$ denotes the complex channel taps for the kth composite signal, $H = H_1 + H_2 + 1$ being the total number of taps, with H_1 pre- and H_2 post-cursor taps. Then, the signal vector is defined as $\mathbf{v}_{k,n} = [v_k[n + H_1] \ \cdots \ v_k[n - H_2]]^T \in \mathbb{C}^{H\times 1}$.

The signal $z[n]$ then undergoes memoryless nonlinear transformation in the PIM source, which in this work is modeled using complex spline-interpolated LUTs [10], [11]. Considering uniform spline interpolation of order P [12], the entries of the LUT are accessed by an index $i[n]$ and abscissa $u[n]$, which are given as

$$i[n] = \left\lfloor \frac{|z[n]|}{\Delta} \right\rfloor + 1; \qquad u[n] = \frac{|z[n]|}{\Delta} - (i[n] - 1), \tag{3}$$

where Δ is the knot spacing, which divides the LUT into $R = |z[n]|_{max}/\Delta$ regions, where $|z[n]|_{max}$ denotes the maximum amplitude of $z[n]$. The abscissa vector $\mathbf{u}_n \in \mathbb{R}^{(P+1)\times 1}$ is further defined as

$$\mathbf{u}_n = \begin{bmatrix} u[n]^P \ u[n]^{P-1} \ \cdots \ 1 \end{bmatrix}^T. \tag{4}$$

Then, we can write the nonlinearity output $s[n]$ as

$$s[n] = z[n](1 + \mathbf{\Psi}_n^T \mathbf{c}_n), \tag{5}$$

where $\mathbf{c}_n \in \mathbb{C}^{C\times 1}$ denotes the spline control points with $C = R + P$ entries, while $\mathbf{\Psi}_n \in \mathbb{R}^{C\times 1}$ represents the spline basis function vector, given as

$$\mathbf{\Psi}_n = \begin{bmatrix} 0 \ \cdots \ 0 \ \mathbf{u}_n^T \mathbf{C}_P \ 0 \ \cdots \ 0 \end{bmatrix}^T, \tag{6}$$

where the first element of the vector $\mathbf{u}_n^T \mathbf{C}_P \in \mathbb{R}^{1\times(P+1)}$ is indexed at $i[n]$. The coefficient matrix $\mathbf{C}_P \in \mathbb{R}^{(P+1)\times(P+1)}$ is determined separately for each interpolation order P, and are defined up to order $P = 4$ in [10].

After the nonlinear transformation, the signal $s[n]$ propagates to the RX antenna to produce the interfering signal, which can be modeled as

$$y[n] = \mathbf{w}_n^T \mathbf{s}_n, \tag{7}$$

where $\mathbf{w}_n \in \mathbb{C}^{M\times 1}$ collects the M channel taps, where $M = M_1 + M_2 + 1$, with M_1 pre- and M_2 post-cursor taps. The signal vector is then defined as $\mathbf{s}_n = [s[n + M_1] \ \cdots \ s[n - M_2]]^T \in \mathbb{C}^{M\times 1}$. Since $y[n]$ now contains also the carrier signals, as illustrated in Fig. 2, a static low-pass filter $\mathbf{b}$ with length $B = B_1 + B_2 + 1$ limits the bandwidth to produce a bandlimited model signal $\hat{y}[n]$ at $-3\omega_0$ as

$$\hat{y}[n] = \mathbf{b}^T \mathbf{y}_n, \tag{8}$$

where $\mathbf{y}_n = [y[n + B_1] \ \cdots \ y[n - B_2]]^T \in \mathbb{C}^{B\times 1}$, while B_1 and B_2 denote the number of pre- and post-cursor taps of the filter $\mathbf{b}$, respectively. Lastly, the PIM distortion is mitigated from the received signal $d[n]$ by a simple subtraction as

$$e[n] = d[n] - \hat{y}[n]. \tag{9}$$

B. Parameter Adaptation

The tracking of the changes in the system is carried out by adapting the filters $\mathbf{h}_{k,n}$, for $k = 1, 2, \cdots, K$, and $\mathbf{w}_n$, and the spline controls points $\mathbf{c}_n$. In order to develop low complexity learning models, we employ the least mean squares (LMS) approach, where the coefficients are updated along the negative direction of the gradient of the cost function $J = e[n]e^*[n]$ [13]. We assume that the rate of change is low for the coefficient vectors. Omitting the full derivations, the update for the linear filter coefficient vector $\mathbf{w}_n$ can be written as

$$\mathbf{w}_{n+1} = \mathbf{w}_n + \mu_w e[n] \mathbf{S}_n^* \mathbf{b}, \tag{10}$$

where $\mathbf{S}_n = [\mathbf{s}_{n+B_1} \ \cdots \ \mathbf{s}_{n-B_2}] \in \mathbb{C}^{M\times B}$, and μ denotes the learning rate. Similarly, the spline control point vector $\mathbf{c}_n$ update is given as

$$\mathbf{c}_{n+1} = \mathbf{c}_n + \mu_c e[n] \mathbf{\Pi}_n^* \mathbf{b}. \tag{11}$$

Table 1. Computational complexity of the proposed cancellation method and the reference models from [9].

Operation	Complexity (FLOPs/sample)		
	This work	**Full BF [9]** ($K = 2$)	**Ch. Coeff. Est. [9]** ($K = 2$, $N_P = 1$)
Main Path	$10KH + 10M$ $+P^2 + 8P + 22$	$448K_{gmp}M + 320M$ $+408K_{gmp} + 306$	$(32K_{gmp}M + 24M$ $+72K_{gmp} + 50) + 2$
Parameter Adaptation	$2KP^2 + 8KP + 4HK + 10HKM$ $+8K + 18CM + 4\tau(C + H + M) - 2C + 20$	$(25088K_{gmp}^2 + 35840K_{gmp}$ $+12800)M^2$	$(128K_{gmp}^2 + 192K_{gmp}$ $+72)M^2 + 342$

The matrix $\mathbf{\Pi}_n \in \mathbb{C}^{C\times B}$ is defined as

$$\mathbf{\Pi}_n = \left[\mathbf{\Sigma}_{n+B_1}\mathbf{Z}_{n+B_1}\mathbf{w}_{n+B_1} \ \cdots \ \mathbf{\Sigma}_{n-B_2}\mathbf{Z}_{n-B_2}\mathbf{w}_{n-B_2}\right], \tag{12}$$

where $\mathbf{\Sigma}_n = [\mathbf{\Psi}_{n+M_1} \ \cdots \ \mathbf{\Psi}_{n-M_2}] \in \mathbb{C}^{C\times M}$, and $\mathbf{Z}_n = \text{diag}\{z[n+M_1] \ \cdots \ z[n-M_2]\} \in \mathbb{C}^{M\times M}$. Finally, the update of the filter coefficients of $\mathbf{h}_{k,n}$ for $k = 1, 2, \cdots, K$ can be written as

$$\mathbf{h}_{k,n+1} = \mathbf{h}_{k,n} + \mu_h e[n]\mathbf{\Xi}_{k,n}^{*}\mathbf{b}, \tag{13}$$

where the matrix $\mathbf{\Xi}_{k,n} \in \mathbb{C}^{H\times B}$ is defined as

$$\mathbf{\Xi}_{k,n} = \left[\mathbf{\Upsilon}_{k,n+B_1}\mathbf{w}_{n+B_1} \ \cdots \ \mathbf{\Upsilon}_{k,n-B_2}\mathbf{w}_{n-B_2}\right], \tag{14}$$

where $\mathbf{\Upsilon}_{k,n} = [\mathbf{v}_{k,n+M_1}\delta[n+M_1] \ \cdots \ \mathbf{v}_{k,n-M_2}\delta[n-M_2]] \in \mathbb{C}^{H\times M}$, and the elements $\delta[n]$ are determined as

$$\delta[n] = \frac{|z[n]|}{2\Delta}\dot{\mathbf{u}}_n^T\mathbf{C}_P\tilde{\mathbf{c}}_n + \mathbf{\Psi}_n^T\mathbf{c}_n + 1, \tag{15}$$

where $\dot{\mathbf{u}}_n = \left[Pu[n]^{P-1} \ (P-1)u[n]^{P-2} \ \cdots \ 1 \ 0\right]^T \in \mathbb{R}^{(P+1)\times 1}$, and $\tilde{\mathbf{c}}_n$ contains $P+1$ elements of $\mathbf{c}_n$ starting from index $i[n]$.

C. Computational Complexity

The computational complexity of the proposed cancellation method is presented in Table 1 in terms of floating point operations (FLOPs) per processed sample, omitting the complexity of the filtering with the static filter $\mathbf{b}$. This operation is also omitted from the complexity of the full basis function (BF) and channel coefficient estimation reference models from [9] shown in Table 1, where K_{gmp} denotes the envelope lead/lag of the generalized memory polynomial model considered in [9]. To obtain the presented results, it is assumed that a complex multiplication requires 8 FLOPs, as does a square root operation. Here, we consider a knot spacing $\Delta = 1$. In Table 1, it is assumed that $\tau \leq B$ taps around the most significant tap of filter $\mathbf{b}$ are considered in the coefficient updates, which has been shown to reduce computational complexity while retaining high accuracy in the updates [10]. The comparison of the computational complexities with practical parametrizations is assessed in the following section.

III. RF Measurements and Results

The proposed cancellation method was tested with the setup shown in Fig. 3, which employs a dual-TX/RX ($K = 2$) base-station (BS) system – limiting the test cases to only $K = 2$ – and a PIM source within an anechoic chamber, while a PC outside the chamber controls the BS and collects data for post-processing. The PIM source is standard off-the-shelf steel-wool, placed approximately a meter away from the BS. The two TX chains transmit dual-carrier signals with 5 MHz bandwidth (BW) each, which are 5G NR compliant CP-OFDM waveforms. Since the BS operates at band n3, TX frequencies of 1819.0 MHz and 1866.5 MHz are chosen, while the RX chains operate at 1771.5 MHz, which corresponds to the lower third-order intermodulation frequency of the TX frequencies.

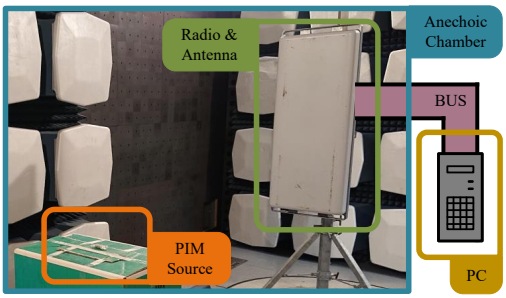

Fig. 3. RF measurement configuration, showing the main parts of the setup.

The signals are oversampled by a factor of 16 to avoid aliasing issues. Similarly, the reference models oversample the signals by a factor of 16 for the BF generation. Otherwise, the following parametrization is adopted unless noted otherwise: $K = 2$, $H = 5$, $P = 2$, $C = 28$ $M = 5$, $\tau = 21$, and $K_{gmp} = 1$. As per Table 1, the complexity per processed sample in the full BF reference model is 4,554 FLOPs in the main path, and 1,843,200 FLOPs in the parameter adaptation, while the channel coefficient estimation model employs 404 FLOPs in the main path and 10,142 FLOPs in learning. In contrast, complexity per sample for the cascaded model proposed in this work is merely 196 FLOPs in the main path with 5 MHz BW, and 6,280 FLOPs in the learning with 5 MHz BW, indicating very significant complexity saving when compared to the reference models. With 20 MHz BW CCs, the proposed canceller has $H = 11$ and $M = 7$, and thus the complexity saving is more moderate: the main path takes 332 FLOPs and the learning 9048 FLOPs. The filters $\mathbf{w}$ and $\mathbf{h}_k$ all employ sparse taps with 20 MHz signals, with every other tap being zero. Then, H and M denote the number of non-zero taps.

Fig. 4 illustrates a power sweep of the achieved cancellation levels w.r.t. the TX power of the carriers – with the reference models of [9] and this work using 5 MHz BW CCs. It can be seen that the proposed model not only matches the performance of the 5th polynomial order reference models, but is capable of outperforming them with high TX powers.

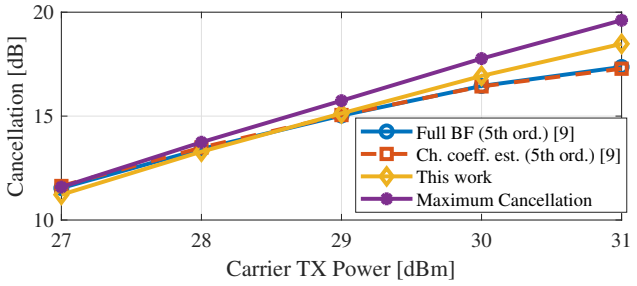

Fig. 4. Achieved cancellation against carrier TX power with 5 MHz CCs.

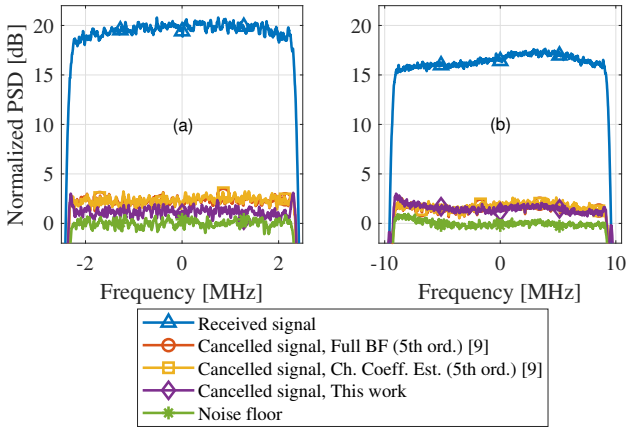

Fig. 5. PSDs of the cancellation result with 5 MHz (a) and 20 MHz (b) BW CC signals at +31 dBm carrier TX power.

For example, with +31 dBm, the reference models achieve around 17.5 dB of cancellation, while the proposed model achieves 18.3 dB. The corresponding power spectral densities (PSDs) of the involved signals in the +31 dBm carrier TX power case are shown in Fig. 5(a). Meanwhile, Fig. 5(b) plots the cancellation results achieved with 20 MHz BW CCs, where the performance of each method is around 14.7 dB. Lastly, Fig. 6 shows the convergence of the proposed cascaded algorithm with both 5 MHz and 20 MHz BW CCs. While the full convergence can be seen to take some 40 ms with both BWs, cancellation level of 15 dB is reached already in around 0.5 ms in the 5 MHz case, while the 20 MHz case achieves suppression of around 8 dB in the same time.

IV. Conclusion

Modeling and cancellation of air-induced PIM in FDD MIMO transceivers based on a Wiener-Hammerstein-type cascaded system was presented in this paper. Unlike previous works, which have considered the rank $K = 2$ case, the introduced cascaded model can handle any rank-K transmission, and potential memory effects in the channels. Further, the provided computational complexity analysis indicates that the proposed model has a greatly reduced complexity compared to the reference models in terms of FLOPS per processed sample. RF measurements conducted with real-life BS equipment evidence that the lowered computational complexity does not compromise the cancellation performance, with the proposed scheme being

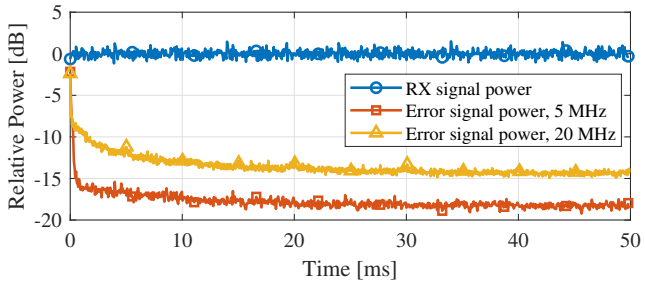

Fig. 6. Convergence of the proposed algorithm, with 5 MHz ($\mu = 0.004$) and 20 MHz ($\mu = 0.002$) BW CC signals at +31 dBm carrier TX power.

able to even outperform the reference models in high TX power scenarios.

Acknowledgment

This work was supported by Nokia Mobile Networks, and by the Academy of Finland under the grants #319994, #323461, and #338224.

References

[1] 3GPP Tech. Spec. 38.104, "NR; Base Station (BS) Radio Transmission and Reception," *v17.7.0, (Release 17)*, September 2022.

[2] Q. Jin, J. Gao, H. Huang, and L. Bi, "Mitigation Methods for Passive Intermodulation Distortion in Circuit Systems Using Signal Compensation," *IEEE Microw. Wireless Compon. Lett.*, vol. 30, no. 2, pp. 205–208, 2020.

[3] X. Chen, T. Ren, D. J. Pommerenke, and M. Yu, "Broadband Mechanical Intermodulation Tuner Using Reconfigurable Distributed Nonlinearity," *IEEE Trans. Microw. Theory Techn.*, vol. 70, no. 1, pp. 5–13, 2022.

[4] J. Henrie, A. Christianson, and W. J. Chappell, "Engineered Passive Nonlinearities for Broadband Passive Intermodulation Distortion Mitigation," *IEEE Microw. Wireless Compon. Lett.*, vol. 19, no. 10, pp. 614–616, 2009.

[5] E. A. Keehr and A. Hajimiri, "Successive Regeneration and Adaptive Cancellation of Higher Order Intermodulation Products in RF Receivers," *IEEE Trans. Microw. Theory Techn.*, vol. 59, no. 5, pp. 1379–1396, 2011.

[6] H.-T. Dabag, H. Gheidi, S. Farsi, P. S. Gudem, and P. M. Asbeck, "All-Digital Cancellation Technique to Mitigate Receiver Desensitization in Uplink Carrier Aggregation in Cellular Handsets," *IEEE Trans. Microw. Theory Techn.*, vol. 61, no. 12, pp. 4754–4765, 2013.

[7] H. Gheidi, H.-T. Dabag, Y. Liu, P. M. Asbeck, and P. Gudem, "Digital Cancellation Technique to Mitigate Receiver Desensitization in Cellular Handsets Operating in Carrier Aggregation Mode with Multiple Uplinks and Multiple Downlinks," in *Proc. 2015 IEEE Radio and Wireless Symposium (RWS)*, 2015, pp. 221–224.

[8] M. Z. Waheed, D. Korpi, L. Anttila, A. Kiayani, M. Kosunen, K. Stadius, P. P. Campo, M. Turunen, M. Allén, J. Ryynänen, and M. Valkama, "Passive Intermodulation in Simultaneous Transmit–Receive Systems: Modeling and Digital Cancellation Methods," *IEEE Trans. Microw. Theory Techn.*, vol. 68, no. 9, pp. 3633–3652, 2020.

[9] V. Lampu, L. Anttila, M. Turunen, M. Fleischer, J. Hellmann, and M. Valkama, "Air-Induced Passive Intermodulation in FDD MIMO Systems: Algorithms and Measurements," *IEEE Trans. Microw. Theory Techn.*, vol. 71, no. 1, pp. 373–388, 2023.

[10] P. Pascual Campo, L. Anttila, D. Korpi, and M. Valkama, "Cascaded Spline-Based Models for Complex Nonlinear Systems: Methods and Applications," *IEEE Trans. Signal Process.*, vol. 69, pp. 370–384, 2021.

[11] T. Paireder, C. Motz, and M. Huemer, "Spline-Based Adaptive Cancellation of Even-Order Intermodulation Distortions in LTE-A/5G RF Transceivers," *IEEE Trans. Veh. Technol.*, vol. 70, no. 6, pp. 5817–5832, 2021.

[12] C. De Boor, *A Practical Guide to Splines*. Springer-Verlag New York, 1978.

[13] S. Haykin, *Adaptive Filter Theory*, 3rd ed. Prentice Hall, 1996.